o-B_2N_2: A Promising Metal-free Photocatalyst for Highly Efficient Conversion of CO_2 to Hydrocarbons

Rajesh Chitara [a), b)], Himalay Kolavada, [a), b)], Madhu Menon [c),d)],

P.N. Gujjar, [b), *] and Sanjeev K. Gupta[a), *]

[a)] Computational Materials and Nanoscience Group, Department of Physics and Electronics, St. Xavier's College, Ahmedabad 380009, India

[b)] Department of Physics, University School of Sciences, Gujarat University, Ahmedabad 380009, India

[c)] Conn Center for Renewable Energy, University of Louisville, Louisville, Kentucky 40292, USA

[d)] Department of Physics and Astronomy, University of Kentucky, Lexington, Kentucky 40506, USA

***Corresponding authors**: Dr Sanjeev K. Gupta (E-mail: sanjeev.gupta@sxca.edu.in) and Prof. P. N. Gajjar (E-mail: pngajjar@gujaratuniversity.ac.in)

Keywords: Density functional theory (DFT), Photocatalysis, CO_2 capture, 2D Boron Nitride, carbon dioxide reduction reaction

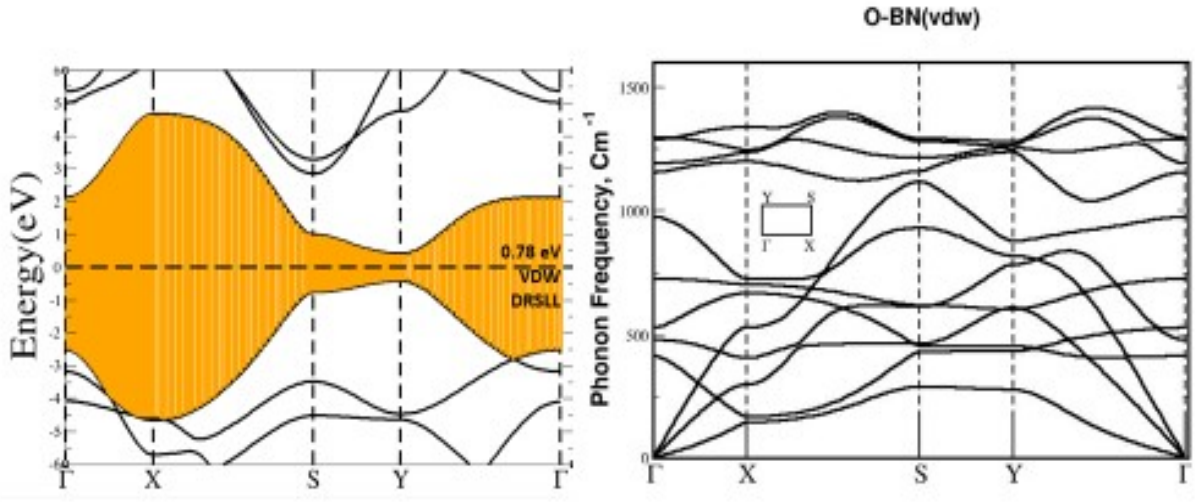

Figure S1. Band structure (left) and phonon dispersion curves (right) of the unit cell of orthorhombic boron nitride along the high symmetry points Γ-X-S-Y-Γ. The band gap at the Y point is 0.78 eV. Positive phonon frequencies suggests dynamic stability of the structure.

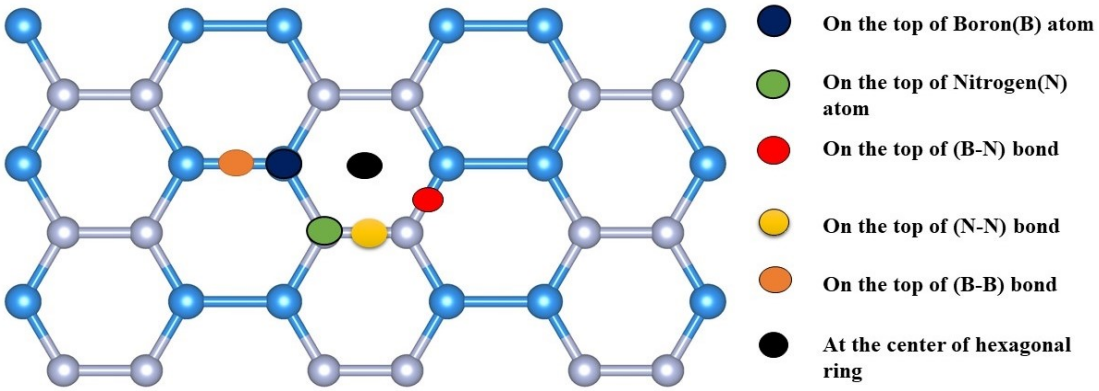

Figure S2. Six possible adsorption sites on the surface of the o-B_2N_2 monolayer. Boron and nitrogen atoms are shown in blue and white, respectively.

Horizontal active sites

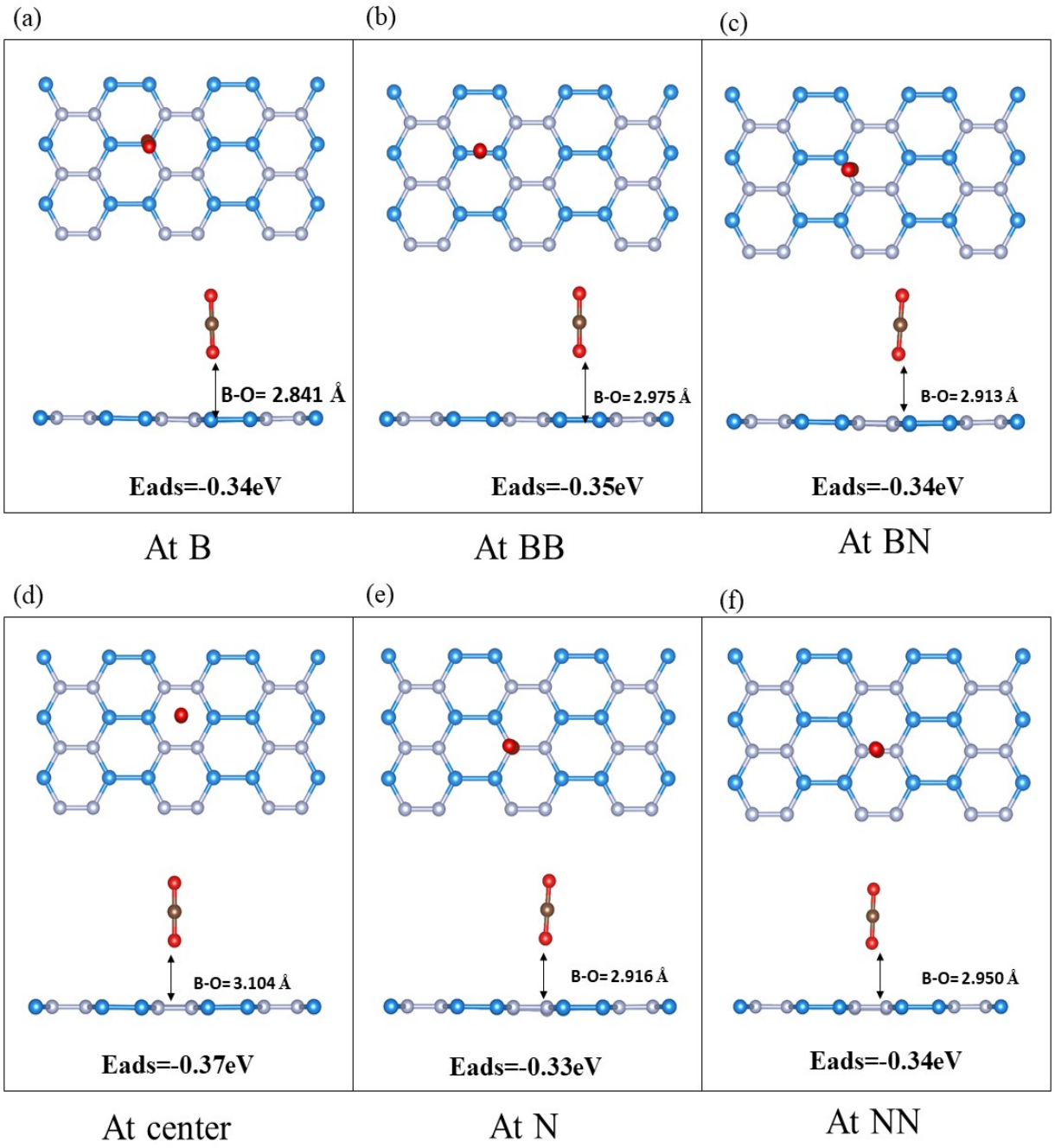

Figure S4 Optimized geometries of CO_2 molecule adsorbed over pristine orthorhombic boron nitride (o-B_2N_2) when CO_2 molecule interacts vertically over the six available active sites. (E_{ads}) represent the corresponding adsorption energies. The distance between the monolayer is indicated with arrow.

Table S1. Initial (I) and final (F) height, change in the angle, and bond length of CO_2 for the desorption of CO_2 over pristine o-B_2N_2 monolayer.

No of site	Active site	Adsorption Energy (eV)	Height (Å) I	Height (Å) F	Angle (degree)	C-O=1.179 (Å)
Site 1	At B	-0.412865	2.115	3.113	179.8	1.186
Site 2	At N	-0.425283	2.011	3.126	180	1.185
Site 3	At B-B	-0.402461	2.191	3.245	179.6	1.185
Site 4	At B-N	-0.430514	2.152	3.173	1.185	1.185
Site 5	At N-N	-0.404501	2.177	3.291	179.8	1.186
Site 6	At center	-0.413672	2.491	3.424	179.7	1.185
		Vertically active sites				
Site 7	At B	-0.347096	2.036	2.841	179.9	1.185
Site 8	At N	0.339909	2.032	2.916	179.9	1.185
Site 9	At B-B	-0.349769	2.191	2.975	180	1.184
Site 10	At B-N	-0.349809	2.193	2.913	179.9	1.182
Site 11	At N-N	-0.34554	2.139	2.95	180	1.186
Site 12	at center	-0.370259	2.516	3.104	180	1.182

Table S2. Calculated structural, adsorption, and electronic parameters of B-, N-, and BN-vacancy defected o-B_2N_2 monolayer before and after CO_2 adsorption. Here H and V denotes horizontal and vertical adsorptions, respectively.

A defective monolayer of O-B_2N_2		Bond length(Å)			CO_2 adsorbed at a Distance (Å)	$E_g(eV)$	Adsorption Energy of CO_2(eV)
		B-B	N-N	B-N			-
Pristine O-BN		1.72	1.45	1.44	-	0.78	-
B vacancy		1.69	1.41	1.38	-	Metallic	-
N vacancy		1.74	1.45	1.42	-	Metallic	-
BN vacancy		1.86	1.60	1.50	-	1.33	-
CO_2 adsorbed over Pristine		1.72	1.45	1.44	3.425	0.78	-0.41
CO_2 adsorbed over B vacancy	H	1.745	1.414	1.45	1.354	0.0008	-3.7516
	V	1.698	1.414	1.404	2.656	0.0236	-0.3540
CO_2 adsorbed over N vacancy	H	1.728	1.447	1.441	3.012	0.0064	-0.3815
	V	1.728	1.450	1.442	2.562	0.0073	-0.3835
CO_2 adsorbed over BN vacancy	H	1.868	1.603	1.445	2.989	1.325	-0.4358
	V	1.868	1.609	1.445	2.585	1.337	-0.3748

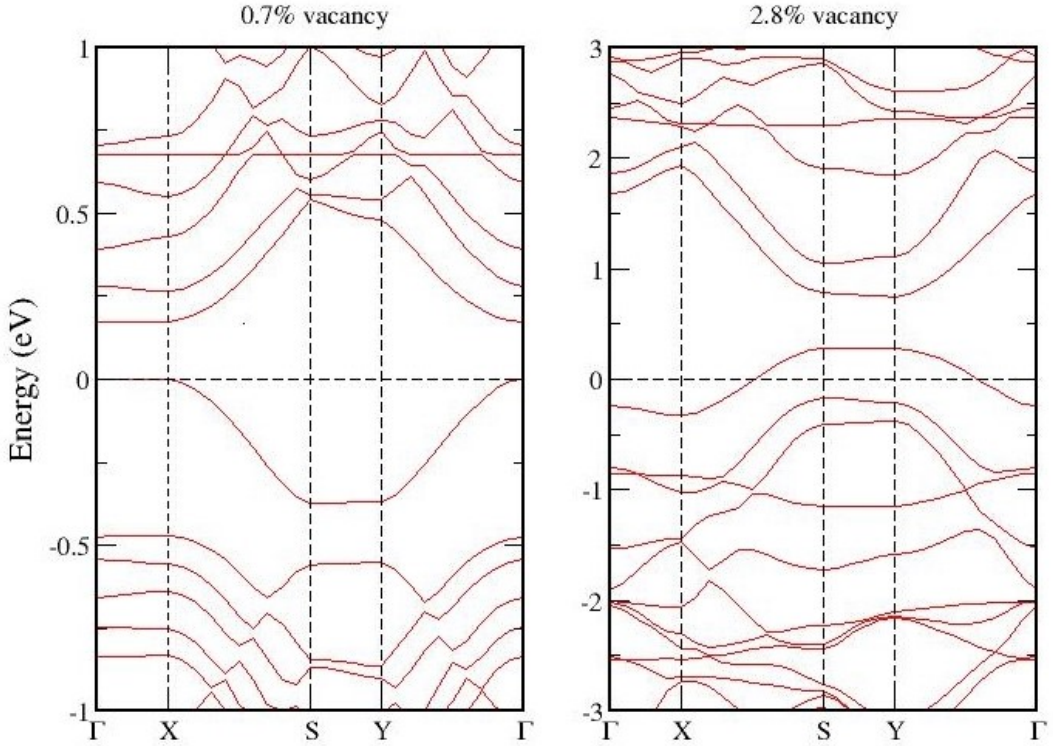

Figure S5. Band structures of SV-B vacancy defected o-B_2N_2 monolayers for two different vacancy concentrations. The Fermi level is set at 0 eV.

Computation Details for defects for Figure S5:

For our *ab initio* calculations we used the density functional theory (DFT) at the level of the generalized gradient approximation (GGA) and the Perdew-Burke- Ernzerhof (PBE)\ as as implemented in the Vienna *Ab-initio* Simulation Package (VASP) [1-4]. The projected augmented wave (PAW) potential is used to describe the core electrons. A kinetic energy cutoff of 520 eV was found to be sufficient to achieve a total energy convergence of the energies of the systems to within 1 meV. Gaussian smearing of 0.05 eV was chosen to accelerate the electronic convergence. The optimization of atomic positions (including full cell optimization) was allowed to proceed without any symmetry constraints until the force on each atom is less than 5 meV/A. In order to assess the effect of the vacancy concentration on the electronic properties we considered two vacancy defected o-BN structures: (i) one shown in Fig 1(a) and, (ii) a much larger 6x6x1 supercell, each containing a single B vacancy giving us defect concentrations of 2.8% and 0.7%, respectively. The k-point sampling was set to be 14 × 14 × 1 for the former, while Gamma point was used for the latter. The supercells are taken to be periodic in the XY-plane with planes separated by 10 Å along the z-direction to avoid interactions between the planes. The band structures obtained using the VASP code is shown

in Figure S5 for the two structures. In the smaller unit cell, the defect-defect interaction causes extended states to develop in the band gap producing metallic behavior, while in the larger supercell the defects are sufficiently far apart to interact with each other and as a result, more bulk like (semiconducting) behavior is seen.

References:

1. G. Kresse and J. Furthmüller, *Phys. Rev. B: Condens. Matter Mater. Phys.*, 1996, **54**, 11169
2. G. Kresse and D. Joubert, *Phys. Rev. B: Condens. Matter Mater. Phys.*, 1999, **59**, 1758
3. W. Kohn and L. J. Sham, *Phys. Rev. A: At., Mol., Opt. Phys.*, 1965, **140**, 1133
4. J. P. Perdew, K. Burke and M. Ernzerhof, *Phys. Rev. Lett.*, 1996, **77**, 3865

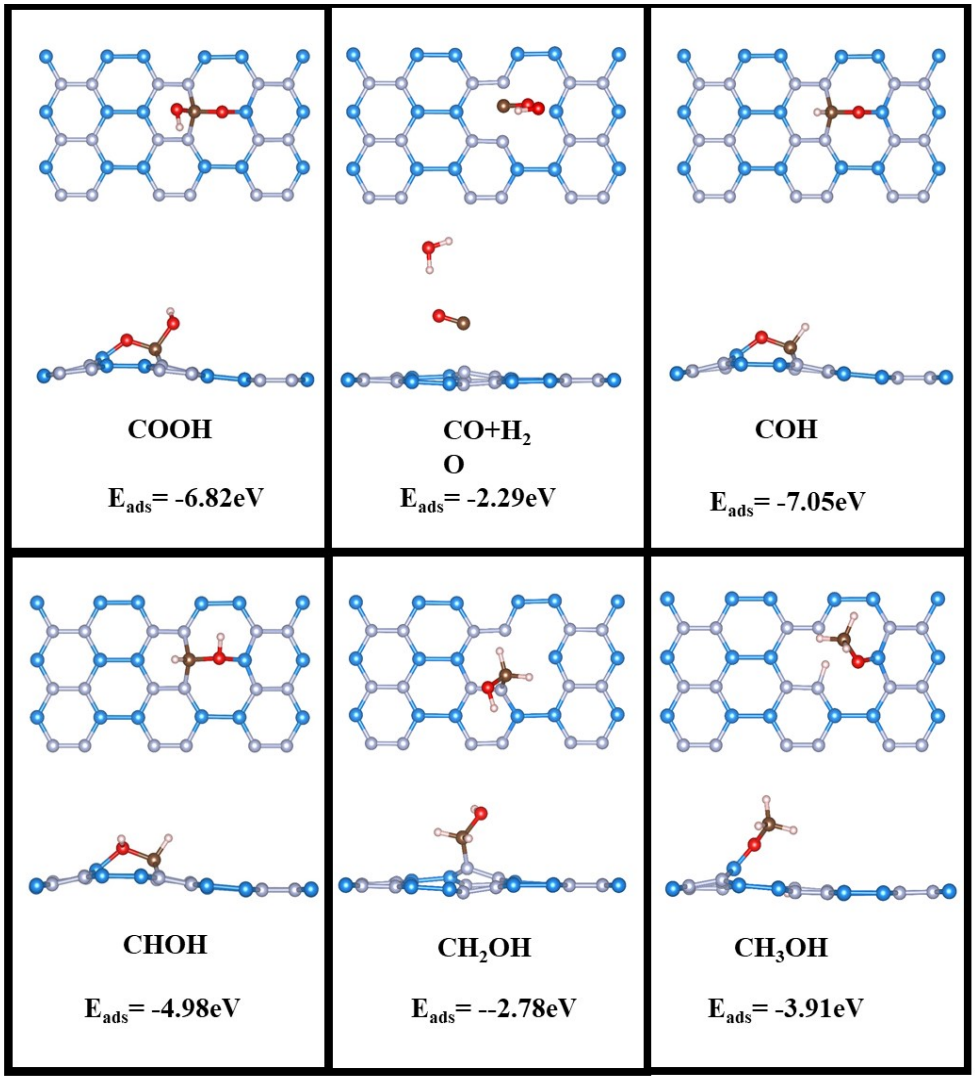

Figure S6. Optimized geometric structures of the adsorption of CO_2 molecule and formation of various intermediates on the surface of 2D monolayer SV-B vacancy-defected o-B_2N_2 material with the equilibrium structures of COOH path.

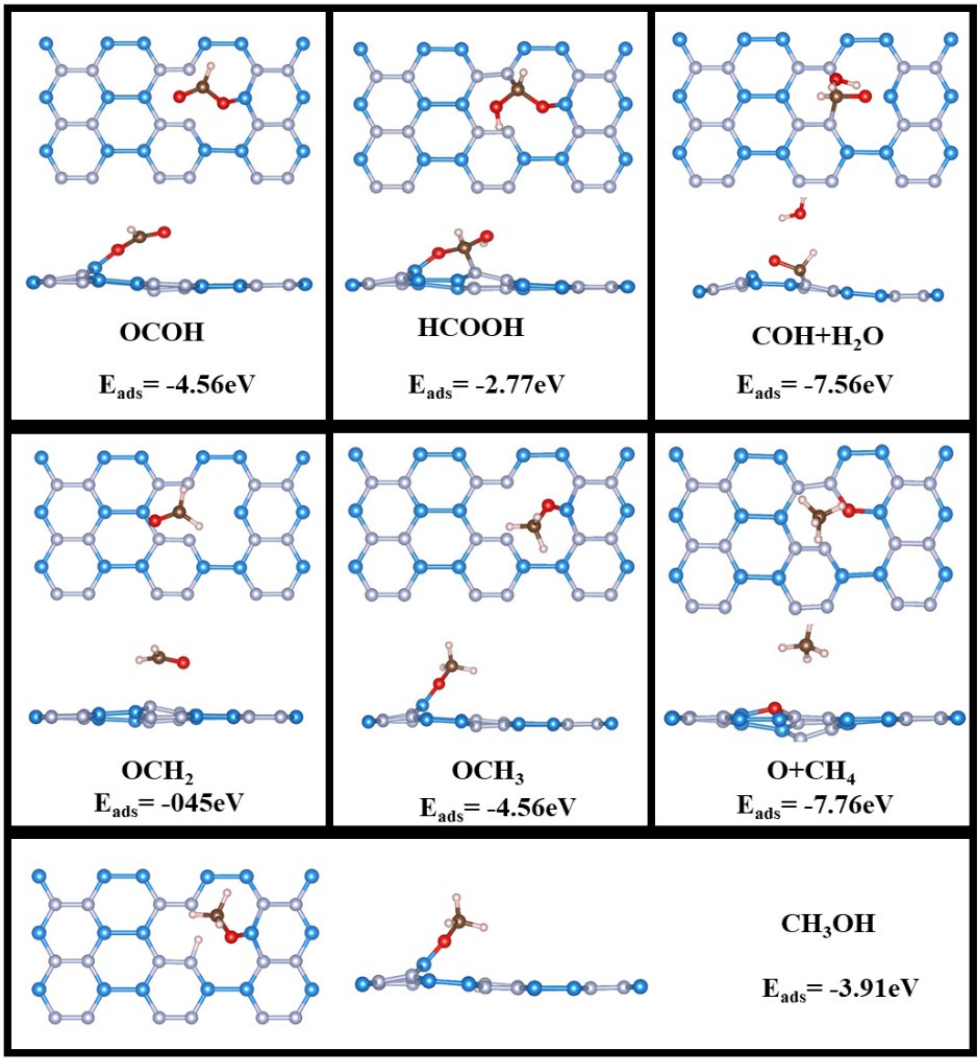

Figure S7. Optimized geometric structures of the adsorption of CO_2 molecules and formation of various intermediates on the surface of 2D monolayer SV-B vacancy-defected o-B_2N_2 material with the equilibrium structures of OCOH path

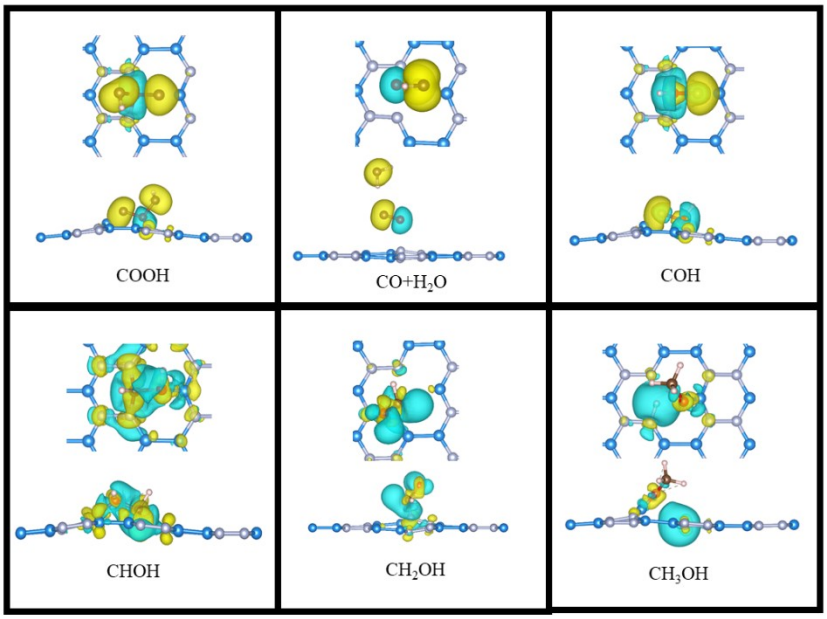

Figure S8. Electron charge density plots of SV-B vacancy defected o-B_2N_2 material and all intermediates formed along the COOH path during the CO_2RR process.

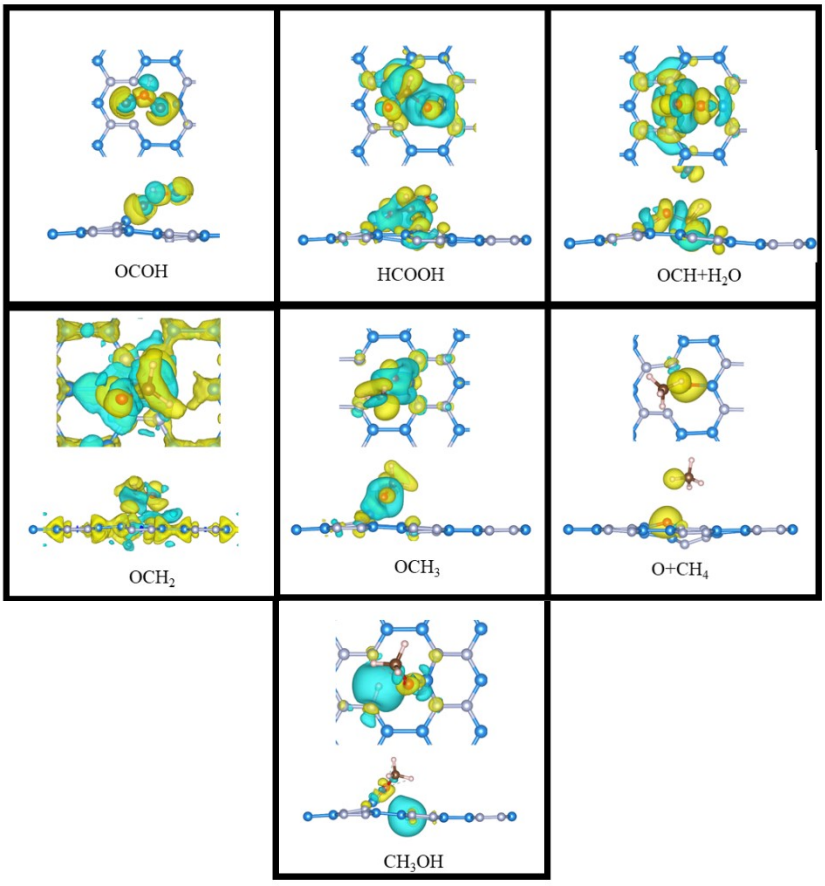

Figure S9. Electron charge density plots of SV-B vacancy defected o-B_2N_2 monolayer and all intermediates formed along the OCOH path during the CO_2RR process.

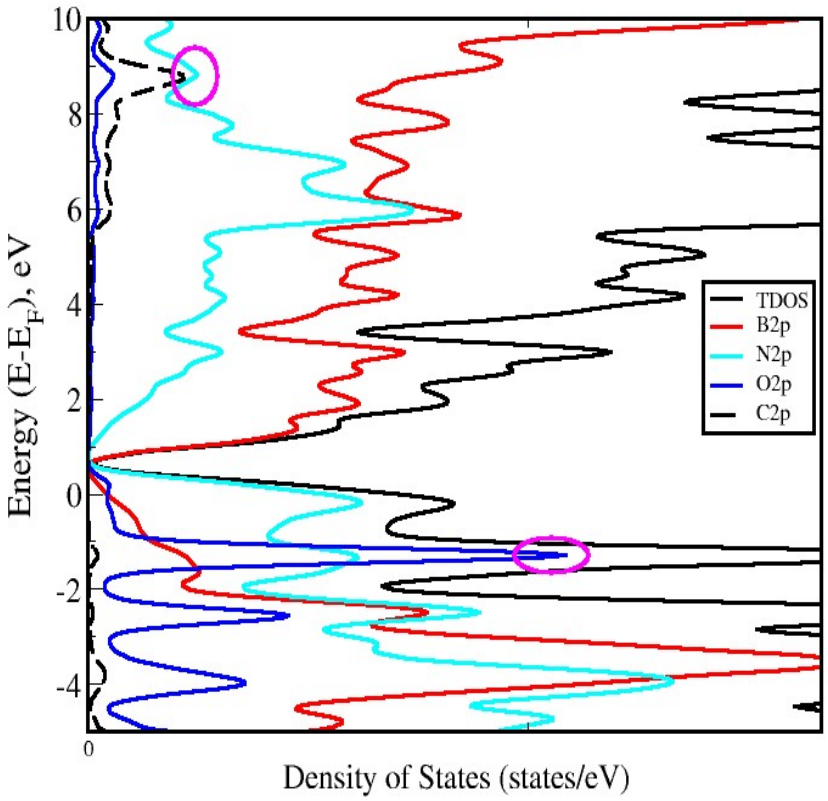

Figure S10. Shows total and projected DOS of horizontal CO_2 adsorption over B-vacancy defected o-B_2N_2 monolayer.